Journal of Emerging Technologies and Industrial Applications
Vol. 5 No. 1 (2026) pp. 1-14
e-ISSN: 2948-507X

Journal homepage: https://jetia.mbot.org.my/index.php/jetia/index

Controlling Water States in UV LED Curable Polyacrylamide Hydrogels: A Pathway to Stronger Biomaterials

Muhammad Aqil Mohd Farizal[1,a], Nadia Adrus[*1,2,b], Nur Amanina Abdul Khalid[1,c], Nurul Balqis Mohamed[1,d], Jamarosliza Jamaluddin[1,3,e]

[1]Department of Chemical Engineering, Faculty of Chemical and Energy Engineering, Universiti Teknologi Malaysia, 81310 UTM Johor Bahru, Johor, MALAYSIA

[2]IJN-UTM Cardiovascular Engineering Centre, Institute of Human Centered Engineering, Universiti Teknologi Malaysia, 81310 UTM Johor Bahru, Johor, MALAYSIA

[3]Institute of Bioproduct Development, Universiti Teknologi Malaysia, 81310 UTM Johor Bahru, Johor, MALAYSIA

Email: [a]m.aqil@graduate.utm.my, [b]nadia@utm.my, [c]amaninakhalid@gmail.com, [d]nurulbalqismohamed@gmail.com, [e]jamarosliza@utm.my

Abstract: Hydrogels, particularly composed of polyacrylamide (PAAm), are extensively utilized for biomaterials, especially in biomedical diagnostics. In biomaterials, the water state is one of the requirements to be eligible for medical use. In this study, PAAm hydrogels were synthesized using UV LED photopolymerization to investigate the effect of the PAAm hydrogel water state towards its overall monomer concentration. This study establishes the direct transition between free water dominant states in low crosslinked networks to non-freezable bound water in highly crosslinked hydrogels, by varying the overall monomer concentration (OMC). The PAAm hydrogel exhibits high monomer conversion efficiency (98%) and high gel fraction (80%) when increasing the OMC. Additionally, the mechanical testing demonstrated that higher OMC enhanced tensile strength by a factor of 6 and Young's modulus by a factor of 13, confirming the formation of a denser polymer network. However, the elongation at break decreased from 63 to 11%, indicating reduced flexibility. Meanwhile, the toughness increased up to 1104 J/m² for 40 wt.% of OMC, while 50 wt.% OMC resulted in brittleness due to excessive crosslinking. The swelling behavior is more controlled for higher OMC (40 – 50 wt.%) due to lower water uptake. From the thermal approach via differential scanning calorimetry analysis, the water states of the hydrogel are determined, where the free water was almost eliminated and left with non-freezable bound water for a highly crosslinked and rigid network at 40 – 50 wt.% of OMC. Further increasing the OMC to 50%, however, results in brittleness and reduced toughness. Therefore, higher OMC (40%) exhibits hydrogels with higher mechanical strength and controlled swelling behavior. These findings introduce valuable insights for designing mechanically robust hydrogels by modifying water hydrogel interaction, a potential method for next-generation biomaterials for tissue adhesives, drug delivery, and biomedical diagnostics, with superior mechanical strength, durability and hydration control.

Received 10 February 2026; Accepted 01 May 2026; Available online 26 June 2026

Keywords: Polyacrylamide hydrogel; UV LED curing; crosslinked polymer network; bound and free water; overall monomer concentration.

*Corresponding Author:
Nadia Adrus,
Department of Chemical Engineering,
Faculty of Chemical and Energy Engineering,
Universiti Teknologi Malaysia,
81310 UTM Johor Bahru, Johor, MALAYSIA
Email: nadia@utm.my

Journal of Emerging Technologies and Industrial Applications
Vol. 5 No. 1 (2026) pp. 1-14
e-ISSN: 2948-507X

Journal homepage: https://jetia.mbot.org.my/index.php/jetia/index

1. Introduction

Hydrogel is a highly hydrophilic three-dimensional (3D) crosslinked network gel polymer structure, which exhibits high water content. Furthermore, hydrogels are widely used in various fields of biomedical diagnostics [1, 2], sensor and actuators [3, 4], energy [5] and medical devices [6]. Their physical attributes including softness, wettability, flexibility, and rubber-like consistency closely mimic natural tissues. The transparency and biocompatibility of hydrogel make them highly effective as biomaterials [7]. Recently, studies have focused on the application of hydrogels as sensor materials in medical diagnostics, for conditions like Parkinson's disease and hemiplegia [6]. This growing interest stems from their unique properties, such as stretchability, self-healing and biodegradability, which enable hydrogels to exhibit high robustness and repeatability under varying degrees of mechanical deformations.

Among various hydrogel systems, polyacrylamide (PAAm) hydrogels formed by the crosslinking of acrylamide (AAm) have attracted significant interest as biomaterials due to their hydrophilic nature, swelling capacity, and improved stretchability [8]. Traditionally, PAAm hydrogels are produced by polymerizing AAm with a bifunctional crosslinking agent, commonly *N, N′*-methylenebisacrylamide (MBAAm). Despite their high water absorption and soft gel formation, these hydrogels typically exhibit low mechanical strength [9]. Recently, UV LED photopolymerization has been recognized as an effective method for synthesizing PAAm hydrogels, achieving monomer conversion rates above 80%. This technique offers advantages such as rapid curing, minimal heat generation, reduced volatile organic compound emissions, and lower operational costs compared to conventional mercury-based UV (UV Hg) systems [10, 11].

Since water is the primary component of hydrogels, it significantly influences their properties, particularly chain flexibility. Studies have classified water within hydrogel networks into bound and unbound states. Based on thermodynamic interactions, three types of water are identified: (i) non-freezable bound water, which is tightly hydrogen-bonded to the polymer and lacks a detectable phase transition; (ii) freezable bound water, which interacts weakly with the hydrogel network and displays altered melting and crystallization points compared to bulk water; and (iii) free water, which does not bond with the hydrogel and exhibits melting and crystallization behavior similar to bulk water. The latter two types are collectively referred to as freezable water [12, 13]. Techniques such as Fourier transform infrared (FTIR) spectroscopy and differential scanning calorimetry (DSC) have been utilized to investigate water states in hydrogels.

The swelling and mechanical characteristics of hydrogels are largely influenced by their gel complexity. While higher gel complexity reduces swelling, it enhances chain flexibility. Previous studies have examined the relationship between water states and swelling behavior, revealing that water molecules strongly bind to the amide

groups of PAAm hydrogels. However, limited research has explored the direct correlation between bound water states and the swelling and tensile properties of PAAm hydrogels [7, 8]. This study introduces a novel approach to enhancing PAAm hydrogel performance through a comprehensive evaluation of how water states influence the swelling and mechanical flexibility of highly crosslinked PAAm hydrogels. Based on previous studies, the research has primarily focused on the general swelling characteristics, compared with this study, which offers insights into the quantification of bound and freezable water and water-hydrogel interactions.

The PAAm hydrogels were synthesized using an efficient UV LED photopolymerization technique with Chivacure 300 as the photoinitiator. This approach ensures a rapid curing process with minimal energy consumption compared to conventional UV curing methods. By varying the overall monomer concentration (OMC) from 10 to 50 wt%, PAAm hydrogels with high gel complexity and monomer conversion were obtained. The synthesized hydrogels were characterized through their mechanical properties such as tensile strength, Young's modulus, and elongation at break. The total organic carbon (TOC) analysis, FTIR spectroscopy, gel fraction measurements, and swelling tests were conducted to evaluate the monomer conversion, functional group, crosslinked percentage, and water state of the PAAm hydrogels, respectively. Additionally, DSC analysis was conducted to study the melting behavior of PAAm hydrogels, identifying different water states and their interactions within the polymer network, particularly intra- and intermolecular hydrogen bonding. The presence of functional groups was characterized using FTIR spectroscopy.

Ultimately, the presence of various water states in PAAm hydrogels significantly enhances their swelling and flexibility. These fundamental results suggest that PAAm hydrogels synthesized via UV LED photopolymerization hold great promise as advanced biomaterials. Furthermore, insights into water-hydrogel interactions and gel complexity can facilitate the development of tougher hydrogels for biomedical and industrial applications such as tissue engineering [14], drug delivery [15], and biomedical diagnostics [1].

2. Materials and Method

AAm with 99 % purity was purchased from Acros Organics (stock from Belgium). MBAAm as a crosslinking agent was purchased from Sigma-Aldrich. "Type I" photoinitiator; commercially known as Chivacure 300 was supplied from Chitec Technology Corp. (Taiwan). Ethanol (Fischer Scientific, 96 % purity) was used as solvent in this study without further purification.

2.1 Preparation of Polyacrylamide Single Network Hydrogel

A series of PAAm hydrogels with different OMC (10 to 50 wt%) were prepared according to Table 1. At first, AAm monomer was dissolved in distilled water and stirred for 5 min. Then, MBAAm as a crosslinker was added and continuously stirred for another 20-25 min. The ratio for AAm and MBAAm was fixed at 95:5. Next, the photoinitiator solution was added into AAm/MBAAm mixture. The photoinitiator solution composed of 2 wt% Chivacure 300 with respect to OMC was dissolved into 1.25 mL ethanol.

Table 1 – Formulation of PAAm hydrogels with OMC of 10 to 50 wt% in overall solution

OMC (wt%)	AAm (mol%)	MBAAm (mol%)	Photoinitiator (mol%)
10	1.055	0.056	0.022
15	1.583	0.084	0.033
20	2.110	0.111	0.044
30	3.166	0.167	0.067
40	4.221	0.222	0.089
50	5.276	0.278	0.111

The pre-gel solution was further stirred for 30 min to get a homogenous solution. To start the polymerization, the pre-gel solutions in Table 1 were exposed to UV LED (Hönle AG, Germany) with λ ~ 365 nm for 15 min. The cured hydrogels were removed from the petri dish and were cut for further characterizations.

2.2 Functional Group Analysis

FTIR spectral analysis was conducted using a Perkin Elmer 1600 Infrared spectrometer (USA) to examine the functional groups within the hydrogels. In summary, approximately 2 mg of the hydrogel samples were finely ground with potassium bromide and compressed into pellets. Each spectrum was recorded with a total of 32 scans at a resolution of 2 cm^{-1}, covering the spectral range of 4000-400 cm^{-1}.

2.3 Conversion Test

A TOC analyzer was used to assess the presence of unreacted monomers and other compounds released from the polymerized hydrogel. The cured hydrogel was submerged in distilled water, with the water being replaced every 24 hours over a period of five days. A 100 mL sample was collected each day and was analyzed using TOC. The degree of monomer conversion was determined by calculating the fraction of leached carbon using the following equation:

$$\text{Monomer Conversion (\%)} = \frac{M_{cgel} - M_{wash}}{M_{cgel}} \times 100 \quad (1)$$

where, M_{cgel} is the mass of total carbon in hydrogel while M_{wash} is the mass of carbon after washing.

2.4 Gel Fraction Test

After polymerization, the samples were cut using a hollow puncher (approximately 1.5 inches in diameter) and were dried in an oven at 45 °C for 5 hours. The dried hydrogels were weighed and subsequently immersed in distilled water at a room temperature for 24 hours to remove any uncrosslinked or residual monomer. After the extraction process, the hydrogels were dried at 45 °C for 24 hours in an oven. Once dried, the hydrogels were weighed, and an average value was obtained from five sets of measurements. The gel fraction was determined using the following equation:

$$\text{Gel Fraction (\%)} = \frac{W_d}{W_i} \times 100 \quad (2)$$

where W_d is the mass of dried hydrogel after extraction, while W_i is the mass of hydrogel before extraction.

2.5 Swelling Analysis

The hydrogel samples were soaked in distilled water at room temperature for 24 hours. Excess surface water was carefully removed using filter paper. The swollen hydrogels were then weighed before being dried in an oven at 80 °C for 24 hours. After drying, the hydrogels were weighed again, and an average value was obtained from five sets of

measurements. The swelling degree was determined using the following formula:

$$\text{Sweling Degree (\%)} = \frac{\text{Mass of swollen hydrogel}}{\text{Mass of dried hydrogel}} \times 100 \quad (3)$$

2.6 Tensile Test

A tensile test was performed to evaluate the mechanical properties of the polymerized hydrogels. The key properties assessed during the test included tensile strength, elongation at break, stress at specific elongation, elongation at specific stress, stress at yield, and elongation at yield. The tensile test was carried out using a CT3 texture analyzer (Brookfield) to examine the stretchability of the hydrogel. The crosshead speed was set between 0.5 and 100 mm/s, with an applied load of 10 kN. The hydrogel samples were cut into rectangular shapes with the dimensions of 50 mm × 3 mm × 5 mm. All measurements were conducted at room temperature.

2.7 Differential Scanning Calorimetry Measurements

The distribution of different water states in hydrogels was analyzed via DSC (Mettler Toledo model DSC822E) with a liquid nitrogen cooling system. Initially, swollen gel samples were gently blotted with filter paper, cut into pieces, and weighed to approximately 10 mg. The samples were then sealed in hermetic pans. After being cooled to -40 °C, they were heated to 40 °C under a nitrogen atmosphere at a flow rate of 50 mL/min. A uniform cooling and heating rate of 10 °C/min was maintained for all tests. Based on the obtained DSC thermograms, the different water states: free water, freezable bound water, and non-freezable bound water were qualitatively analyzed.

3. Results and Discussion

3.1 Formation of PAAm Hydrogels Induced by UV LED photopolymerization

Figure 1 shows the proposed structure of PAAm hydrogels formed via UV LED photopolymerization and its FTIR spectrum to characterize its functional group. The PAAm hydrogels undergo free-radical polymerization, where AAm monomers are polymerized in the presence of MBAAm as the crosslinker and Chivacure 300 as the photoinitiator. From the FTIR spectrum, a broad absorption band near ~3400 cm^{-1}, with distinct peaks at ~3392 cm^{-1} and ~3195 cm^{-1}, corresponds to the NH stretching vibrations of the amide groups, indicating strong hydrogen bonding interactions within the PAAm network 16. A prominent peak at ~2941 cm^{-1} is assigned to the aliphatic CH stretching vibrations, confirming the presence of hydrocarbon chains in the polymer backbone 6. The hydrocarbon chains are formed via the reaction of bifunctional MBAAm crosslinker with the growing polymer chains derived from the AAm monomers, creating covalent crosslinks that result in a rigid 3D hydrogel network (Figure 1, bottom left). Meanwhile, the characteristic amide I band, attributed to the C=O stretching of amide groups, appears prominently at ~1662 cm^{-1}, which is a signature feature of PAAm hydrogels 16. Additionally, the absorption peaks at ~1612 cm^{-1} and ~1417 cm^{-1} correspond to NH bending and CN stretching vibrations, respectively, further verifying the presence of amide functional groups 16.

In PAAm hydrogels, the amide functional group is crucial in controlling the water states. Strong hydrogen bond is formed with water, where the C=O in the amide group accepts and N-H donates, which promote water uptake and

create non-freezable bound water 17. However, the amount of amide group is affected by the OMC of the PAAm hydrogel, where different OMC may vary the network density and alter the water states in the hydrogel structure, which is further discussed in Section 3.3.3.

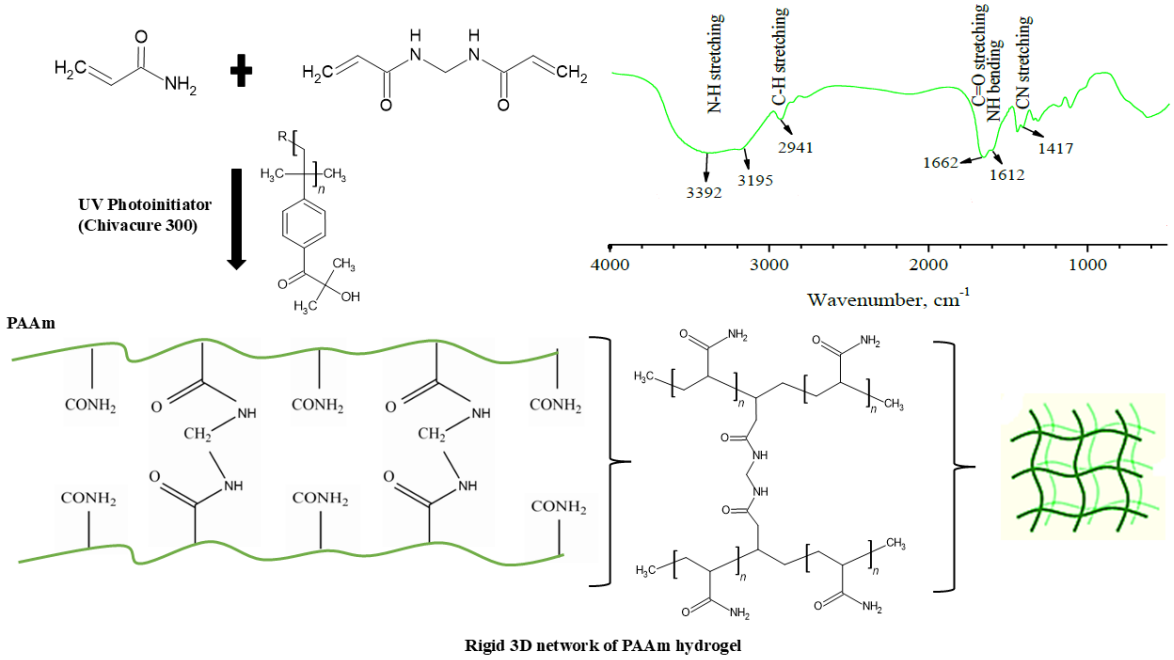

Fig.1- Schematic diagram of PAAm hydrogels formation via UV LED photopolymerization and FTIR analysis of functional groups and the proposed network structure

3.2 Characterization of PAAm Hydrogels

3.2.1 Conversion Test and Gel Fraction

The monomer conversion and gel fraction tests collectively provide crucial insights into the polymerization efficiency and network density of PAAm hydrogels. In Figure 2, the monomer conversion measures the extent to which AAm monomers polymerize, while the gel fraction quantifies the proportion of these monomers that form a stable crosslinked network. From the monomer conversion analysis, it is demonstrated that the PAAm hydrogels exceed 98% conversion across all OMC. This indicates that nearly all of the AAm monomers are successfully polymerized in the presence of MBAAm. The highest monomer conversion of 99.1% is achieved by the hydrogel with 50 wt.% of OMC, and the hydrogel with the lowest OMC (10 wt.%) possessed the least monomer conversion of 98%. However, high monomer conversion does not necessarily mean complete crosslinking, as some polymerized AAm chains may remain linear or only loosely connected rather than integrating into a robust 3D hydrogel network [16-18]. This can be confirmed from the results obtained in Section 3.3.2, where higher OMC (50 wt.%) exhibit a decrease in toughness.

Meanwhile, the gel fraction test revealed an increasing trend from 66% to 82%, as OMC increased. At low OMC (10–20 wt%), the gel fraction remained at around 66%, suggesting a relatively loose network with a significant proportion of linear PAAm chains that polymerized but did not undergo full crosslinking. This is likely due to insufficient monomer and crosslinker concentrations,

which causes a large space formation between the polymer network and limits the interconnected gel structure [19]. As OMC increased to 30–40 wt**%**, the gel fraction rose to 78–80**%**, indicating a more efficient crosslinking process that enhanced hydrogel density and mechanical performance. This range represents an optimal balance between polymerization efficiency and crosslinking density, producing a highly entangled hydrogel with near-perfect elasticity [20]. However, at higher OMC (50 wt%), the gel fraction plateaued at 82**%**, suggesting that further increasing monomer concentration does not proportionally enhance crosslinking. Excessive crosslinking at this stage led to a brittle hydrogel structure with reduced elongation at break**,** likely due to steric hindrance or diffusion limitations preventing uniform network formation [21, 22].

Overall, these findings highlight that while monomer conversion is crucial for efficient hydrogel synthesis, it does not directly dictate crosslinking density. At lower OMC, unreacted linear polymer chains remain, leading to weaker gel structures. As OMC increases, gel fraction improves, forming a denser network that enhances mechanical properties but reduces flexibility at excessive crosslinking densities. Therefore, optimizing OMC is essential to balancing polymerization efficiency, crosslinking density, and the mechanical properties of PAAm hydrogels.

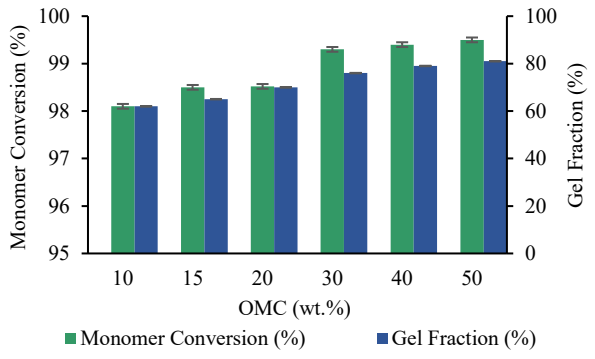

Fig.2- Monomer conversion and gel fraction versus the OMC of PAAm hydrogel

3.2.2 Mechanical Properties

To evaluate these mechanical characteristics, the tensile properties of PAAm hydrogels including tensile strength, Young's modulus, elongation at break, and toughness were examined using a texture analyzer. From the results depicted in Figure 3, increasing the OMC in PAAm hydrogels led to a significant improvement in tensile strength and Young's modulus, from 0.01 MPa to 0.06 MPa and 0.02 MPa to 0.26 ± 0.02 MPa, respectively. At lower OMC (10 to 20 wt%), AAm and MBAAm are dispersed due to the excess amount of water in the hydrogel formulation, and the polymer network formed is sparsely densed. Meanwhile, higher OMC (30 to 50 wt%) resulted in extensively more dense structure, leading to a denser and stiffer network [23]. Therefore, this notable enhancement suggests that the higher OMC concentration exhibits reduced water content, resulting in additional polymer network densities, thereby reinforcing the hydrogel structure.

The hydrogel network structure of lower and higher OMC in PAAm hydrogels are illustrated in Figure 4. It is important to note that as the OMC increased, the structural heterogeneity of PAAm hydrogels also intensified. The complexity of the hydrogel network rises as monomer concentration increases from 10 to 50 wt%. At higher OMC, network density is more likely to happen, which increases the actual crosslinking density since the spatial crosslinks were introduced in addition to the chemically crosslinked polymer chains [24].For hydrogel with high OMC, the segmental lengths between crosslinking points become shorter, and the formation of chain loops becomes more prevalent [25].

Consequently, the applied load is more evenly distributed throughout the polymeric matrix with higher OMC, which improved the tensile strength of the hydrogel [19].

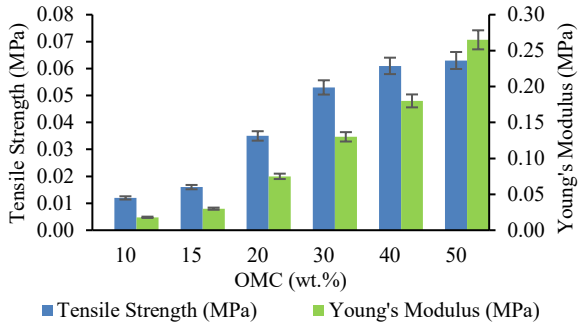

Fig.3- The tensile strength and Young's modulus of PAAm hydrogels as a function of OMC concentration (wt.%)

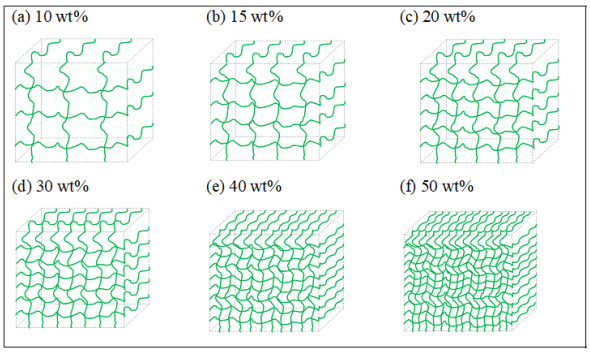

Fig.4- Structures of PAAm hydrogels at various total monomer concentrations

The mechanical properties were further investigated by measuring the elongation at break and toughness of the PAAm hydrogels. The relationship between elongation at break and AAm concentration (ranging from 10 to 50 wt%) is shown in Figure 5. A significant decrease in elongation at break was observed, dropping from 63 ± 5.9% to 11 ± 0.1% as the OMC concentration increased. This decline indicates that higher AAm concentrations lead to greater network entanglement and structural complexity, thereby limiting the flexibility of PAAm chains [26]. Highly crosslinked hydrogels tend to be more rigid and brittle, resulting in lower elongation at break. Additionally, due to the heterogeneous nature of the network, certain polymer chain segments experience higher deformation than others, causing the gel to break at relatively low strain levels [27]. Beyond stretchability, achieving good toughness is crucial for various applications involving soft materials.

Figure 5 also illustrates the toughness of PAAm hydrogels across different OMC. At 40 wt% monomer concentration, the toughness of PAAm hydrogels progressively increased from 439 ± 39.8 J/m² to 1104 ± 90.5 J/m². This enhancement is attributed to the optimized balance of hydrogen bonding interactions between amide groups within the PAAm network, resulting in a tougher hydrogel [28].

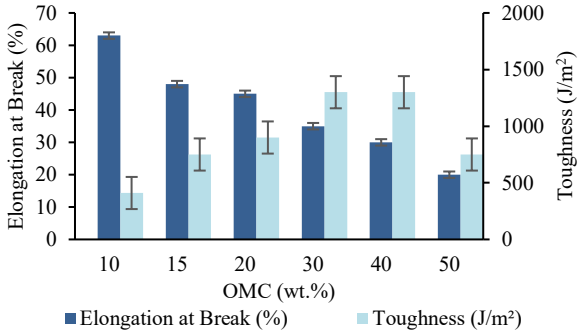

Fig.5- Variation of OMC concentration (wt.%) towards the elongation at break and the toughness of PAAm hydrogel

A tougher hydrogel can dissipate more energy during deformation and fracture, making it more resilient. However, beyond 40 wt% monomer concentration, the toughness of PAAm hydrogels declined to 814 ± 34.6 J/m². This reduction suggests that as the network density continues to rise, amide-amide interactions become more dominant than hydrogen bonding interactions, weakening the toughness of the hydrogel [25]. Furthermore, excessive crosslinking leads to an increasingly

brittle structure, which further diminishes the toughness of the hydrogel.

3.2.3 Water State in Hydrogel

The swelling behavior of the PAAm hydrogels is influenced by the water states within the polymer matrix. Swelling is the ability of the hydrogel to absorb and retain water, while the water states within the hydrogel provide insights into the interaction of water with the polymer network. In Figure 6(a), the swelling of the PAAm hydrogel at low OMC (10 – 20 wt.%) was significantly higher (10.7), indicating a more open and flexible polymer network that allowed for greater water uptake. From the DSC analysis in Figure 6(b), the sharp crystallization peaks at approximately -20°C indicate a large proportion of free water and freezable bound water in the hydrogel structure. As illustrated in Figure 6(c)(i), the increase in swelling capacity of the hydrogel is due to a large amount of free water (blue) and loosely freezable bound water (yellow) within the polymer matrix, The presence of free water further promotes hydrogel expansion as osmotic pressure drives additional water absorption into the polymer matrix [8, 12, 29].

As the OMC increased to 30 wt.% in Figure 6(a), the swelling degree progressively declined. The DSC data in Figure 6(b) revealed a doublet peak between -40 and -20 °C, which indicates the freezable bound water interacting more strongly with the polymer chains. This shift indicates that water molecules were increasingly confined within the hydrogel structure due to enhanced crosslinking, reducing the proportion of free water available for swelling. At this stage, the hydrogel still maintained some degree of flexibility, but the presence of tightly bound water restricted polymer mobility, leading to a moderate decrease in swelling [30, 31]. Hence, more tightly bound water (red) and less freezable bound water in the polymer matrix, as illustrated in Figure 5(c)(ii).

At high OMC (40–50 wt%), swelling behavior stabilized at its lowest values (4.1), reflecting the formation of a rigid network. Correspondingly, the DSC analysis showed the disappearance of endothermic peaks below 0 °C, indicating that free water was almost completely eliminated, leaving only non-freezable bound water. This form of water is tightly integrated within the hydrogel matrix, strongly interacting with hydrophilic functional groups of the polymer and preventing further swelling, as shown in Figure 6(c)(iii). The rigid network significantly restricted the diffusion and absorption of water, leading to minimal expansion upon hydration [32, 33]. From these findings, swelling and water retention in PAAm hydrogels are directly influenced by the polymer network structure, where higher crosslinking density limiting water absorption and reducing overall hydrogel flexibility.

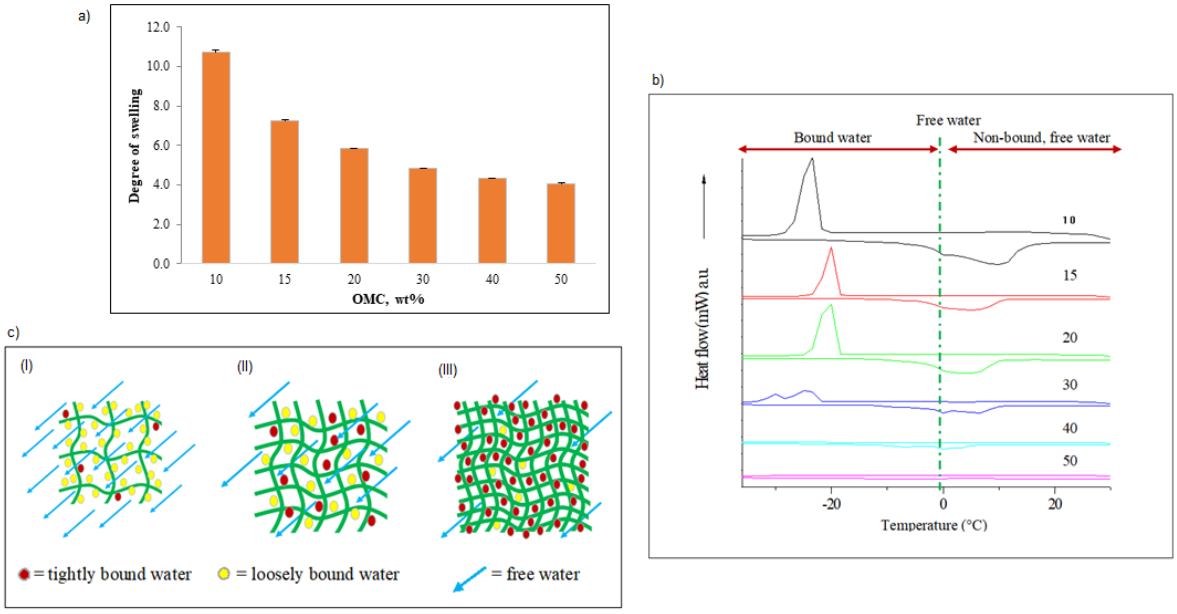

Fig.6- (a) Swelling degree of PAAm hydrogel as a function of OMC, (b) DSC thermograms of different total monomer concentrations of PAAm hydrogel and (c) Proposed illustration of tightly and loosely bound water and mobility of free water in PAAm networks at; (a) low, (b) medium and (c) high crosslinked networks

4. Conclusion

This study successfully developed and analyzed PAAm hydrogels using UV LED photopolymerization, focusing on how different water states influence their swelling and mechanical properties. The results showed that PAAm hydrogels achieved high monomer conversion efficiency (>98%) as the OMC increased, leading to a more tightly crosslinked structure. The gel fraction analysis further confirmed that higher OMC resulted in a stronger and more stable hydrogel network. Besides, the mechanical testing demonstrated that higher OMC led to improved tensile strength and stiffness due to higher polymer network density, making the hydrogel more durable. However, the flexibility is reduced at the highest OMC of 50 wt.%, as shown by the decreasing elongation at break. Interestingly, the hydrogel's toughness peaked at 40 wt% of OMC, beyond which excessive crosslinking made the material more brittle, reducing its ability to absorb energy during deformation. The swelling studies revealed that the polymer network became denser with increasing OMC, reducing the hydrogel's ability to absorb water due to the transition from free water-dominant swelling to a tightly bound, non-freezable water. Furthermore, the DSC analysis supported this observation, showing a shift in water mobility as the crosslinking density increased. These findings highlight the critical relationship between hydrogel structure, water retention, and mechanical performance. By fine-tuning the monomer concentration and crosslinking density, PAAm hydrogels can be optimized for various applications, including biomedical devices, soft robotics, and tissue engineering. Future research could explore the incorporation of secondary polymer networks or functional additives to further enhance hydrogel flexibility and resilience, ensuring their suitability for a wider range of applications.

Acknowledgement

This work was supported by the Universiti Teknologi Malaysia Fundamental Research (UTMFR Vote No. Q.J130000.3846.23H13) funded by Universiti Teknologi Malaysia.

References

[1] Z. Liang *et al.*, "Flexible and self-healing electrochemical hydrogel sensor with high efficiency toward glucose monitoring," *Biosensors and Bioelectronics,* vol. 155, p. 112105, 2020/05/01/ 2020, doi: https://doi.org/10.1016/j.bios.2020.112105.

[2] O. Chaudhuri *et al.*, "Hydrogels with tunable stress relaxation regulate stem cell fate and activity," *Nature Materials,* vol. 15, no. 3, pp. 326-334, 2016/03/01 2016, doi: 10.1038/nmat4489.

[3] Z. Deng, H. Wang, P. X. Ma, and B. Guo, "Self-healing conductive hydrogels: preparation, properties and applications," *Nanoscale,* 10.1039/C9NR09283H vol. 12, no. 3, pp. 1224-1246, 2020, doi: 10.1039/C9NR09283H.

[4] Y. S. Zhang and A. Khademhosseini, "Advances in engineering hydrogels," *Science,* vol. 356, no. 6337, p. eaaf3627, 2017.

[5] C. Yang and Z. Suo, "Hydrogel ionotronics," *Nature Reviews Materials,* vol. 3, no. 6, pp. 125-142, 2018/06/01 2018, doi: 10.1038/s41578-018-0018-7.

[6] Z. Wang *et al.*, "A flexible, stretchable and triboelectric smart sensor based on graphene oxide and polyacrylamide hydrogel for high precision gait recognition in Parkinsonian and hemiplegic patients," *Nano Energy,* vol. 104, p. 107978, 2022/12/15/ 2022, doi: https://doi.org/10.1016/j.nanoen.2022.107978.

[7] J. M. Scalet, T. C. Suekama, J. Jeong, and S. H. Gehrke, "Enhanced Mechanical Properties by Ionomeric Complexation in Interpenetrating Network Hydrogels of Hydrolyzed Poly (N-vinyl Formamide) and Polyacrylamide," *Gels*, vol. 7, no. 3, doi: 10.3390/gels7030080.

[8] R. Kawai, H. Tanaka, S. Matsubara, S. Ida, M. Uchida, and D. Okumura, "Implicit rule on the elastic function of a swollen polyacrylamide hydrogel," *Soft Matter,* vol. 17, no. 19, pp. 4979-4988, 2021.

[9] B. Ehrke, J. Erfkamp, and T. Wallmersperger, "Experimental investigation of the mechanical behavior of a poly (acrylamide-co-sodium acrylate) hydrogel," *Journal of Intelligent Material Systems and Structures,* vol. 33, no. 2, pp. 309-318, 2022.

[10] R. Mansurov *et al.*, "TiO2-embedded biocompatible hydrogel production assisted with alginate and polyoxometalate polyelectrolytes for photocatalytic application," *Inorganics,* vol. 11, no. 3, p. 92, 2023.

[11] Y. Zhang *et al.*, "Preparation and properties of polyester fibers with polyacrylamide hydrogel grafted by UV-irradiation," *Polymer Engineering & Science,* vol. 64, no. 2, pp. 865-874, 2024/02/01 2024, doi: https://doi.org/10.1002/pen.26590.

[12] T. C. P. Bui and N. A. T. Huynh, "Effect of Linear Polyacrylamide on the Properties of semi–IPN Hydrogels Based on N, N'–Dimethylacrylamide, and Maleic Acid," *Journal of Technical Education Science,* vol. 18, no. 6, pp. 24-33, 2023.

[13] A. Jafari, S. Hassanajili, F. Ghaffari, and N. Azarpira, "Modulating the physico-mechanical properties of polyacrylamide/gelatin hydrogels for tissue engineering application," *Polymer Bulletin,* vol. 79, no. 3, pp. 1821-1842, 2022.

[14] H. Yang, C. Li, J. Tang, and Z. Suo, "Strong and Degradable Adhesion of Hydrogels," *ACS Applied Bio Materials,* vol. 2, no. 5, pp. 1781-1786,

2019/05/20 2019, doi: 10.1021/acsabm.9b00103.

[15] J. Li and D. J. Mooney, "Designing hydrogels for controlled drug delivery," *Nature Reviews Materials,* vol. 1, no. 12, pp. 1-17, 2016.

[16] A. Gallastegui *et al.*, "Fast visible-light photopolymerization in the presence of multiwalled carbon nanotubes: Toward 3D printing conducting nanocomposites," *ACS Macro Letters,* vol. 11, no. 3, pp. 303-309, 2022.

[17] S. K. Ghazali, N. Adrus, R. A. Majid, F. Ali, and J. Jamaluddin, "UV-LED as a new emerging tool for curable polyurethane acrylate hydrophobic coating," *Polymers,* vol. 13, no. 4, p. 487, 2021.

[18] H. Ju *et al.*, "Polymerization-induced crystallization of dopant molecules: an efficient strategy for room-temperature phosphorescence of hydrogels," *Journal of the American Chemical Society,* vol. 145, no. 6, pp. 3763-3773, 2023.

[19] Y. Wang, G. Nian, J. Kim, and Z. Suo, "Polyacrylamide hydrogels. VI. Synthesis-property relation," *Journal of the Mechanics and Physics of Solids,* vol. 170, p. 105099, 2023/01/01/ 2023, doi: https://doi.org/10.1016/j.jmps.2022.105099.

[20] J. Kim, G. Zhang, M. Shi, and Z. Suo, "Fracture, fatigue, and friction of polymers in which entanglements greatly outnumber cross-links," *Science,* vol. 374, no. 6564, pp. 212-216, 2021/10/08 2021, doi: 10.1126/science.abg6320.

[21] L. Hong *et al.*, "Tough and self-healing hydrogels based on transient crosslinking by nanoparticles," *Soft Matter,* vol. 18, no. 9, pp. 1885-1895, 2022.

[22] N.-E. Angar and D. Aliouche, "Effect of Ionic Strength, Crosslinking Degree and Copolymerization on Properties of Poly (Acrylamide) Hydrogel, Application as Adsorbent of Heavy Metal Ions," *Journal of Water Chemistry and Technology,* vol. 43, pp. 228-235, 2021.

[23] Z. Li, Z. Liu, T. Y. Ng, and P. Sharma, "The effect of water content on the elastic modulus and fracture energy of hydrogel," *Extreme Mechanics Letters,* vol. 35, p. 100617, 2020/02/01/ 2020, doi: https://doi.org/10.1016/j.eml.2019.100617.

[24] A. P. Safronov, N. M. Kurilova, L. V. Adamova, T. F. Shklyar, F. A. Blyakhman, and A. Y. Zubarev, "Hydrogels Based on Polyacrylamide and Calcium Alginate: Thermodynamic Compatibility of Interpenetrating Networks, Mechanical, and Electrical Properties," *Biomimetics*, vol. 8, no. 3, doi: 10.3390/biomimetics8030279.

[25] Q. Yang *et al.*, "Enhanced mechanical strength of metal ion-doped MXene-based double-network hydrogels for highly sensitive and durable flexible sensors," *ACS Applied Materials & Interfaces,* vol. 15, no. 44, pp. 51774-51784, 2023.

[26] S. Pruksawan *et al.*, "Enhancing hydrogel toughness by uniform cross-linking using modified polyhedral oligomeric silsesquioxane," *Communications Materials,* vol. 4, no. 1, p. 75, 2023/09/27 2023, doi: 10.1038/s43246-023-00402-2.

[27] C. Li, Z. Wang, Y. Wang, Q. He, R. Long, and S. Cai, "Effects of network structures on the fracture of hydrogel," *Extreme Mechanics Letters,* vol. 49, p. 101495, 2021/11/01/ 2021, doi: https://doi.org/10.1016/j.eml.2021.101495.

[28] C.-K. Chen, P.-W. Chen, H.-J. Wang, and M.-Y. Yeh, "Alkyl chain length effects of imidazolium ionic liquids on electrical and mechanical performances of polyacrylamide/alginate-based hydrogels," *Gels,* vol. 7, no. 4, p. 164, 2021.

[29] B. Brundha and P. Pazhanisamy, "Synthesis and Swelling behavior of

Poly (N-tert-amylacrylamide-co–acrylamide/AMPS Na) Nanocomposite Hydrogels," in *ICCM International Conferences on Composite Materials, Jeju Island, South Korea*, 2011.

[30] P. N. Rockwell, J. E. Maneval, B. M. Vogel, and E. L. Jablonski, "Water diffusion and uptake in injectable ETTMP/PEGDA hydrogels," *The Journal of Physical Chemistry B,* vol. 127, no. 22, pp. 5055-5061, 2023.

[31] M. Simeonov, A. A. Apostolov, M. Georgieva, D. Tzankov, and E. Vassileva, "Poly (acrylic acid-co-acrylamide)/polyacrylamide pIPNs/magnetite composite hydrogels: synthesis and characterization," *Gels,* vol. 9, no. 5, p. 365, 2023.

[32] A. Almohsin, M. R. Krishnan, E. Alsharaeh, and B. Harbi, "Preparation and Properties Investigation on Sand-Polyacrylamide Composites with Engineered Interfaces for Water Shutoff Applications," in *SPE Middle East Oil and Gas Show and Conference*, 2023: SPE, p. D021S086R004.

[33] S. Franco, E. Buratti, V. Nigro, M. Bertoldo, B. Ruzicka, and R. Angelini, "Thermal behaviour of microgels composed of interpenetrating polymer networks of poly (N-isopropylacrylamide) and poly (acrylic acid): A calorimetric study," *Polymers,* vol. 14, no. 1, p. 115, 2021.